Research on Aerodynamic Noise Reduction of Rotary Compressor Discharge Port Slope

Yi Zhou[1,2]*, Weikang Jiang[1] , Haijun Wang[2], Shujun Shan[2]

[1]Shanghai Jiaotong University,
Shanghai, China
zhouyishec@126.com

[2]Shanghai Highly Electrical Appliances CO.,LTD,
Shanghai, China

* Corresponding Author

ABSTRACT

Aerodynamic noise is one of the important sound sources of rotary compressors. The airflow velocity is about 20m/s~50m/s near the discharge port when the high pressure refrigerant is discharging , and the airflow impacts the wall, so it forms complex vortexes, which generates aerodynamic noise. Therefore it is necessary to reduce the noise source near the discharge port of main bearing in rotary compressors. The discharge slope is redesigned, VG, serration and Helmholtz resonance chamber structure are used to control the flow. The 3D unsteady turbulent simulation is performed with DES method, then the dipole noise field is simulated using Simcenter3D. The CFD simulations show that VG and serrations help to reduce the turbulent kinetic energy in the muffler, FFT of the pressure at the muffler outlets shows a significant decrease in the pressure amplitude at 400,1000 Hz frequency interval. The Helmholtz resonance chamber works in a wider range than the design point. 3 compressors are manufactured for each scheme, the pressure at discharge port and sound power are tested. The test results show that the VG scheme reduces about 2dB in 1kHz frequency interval, and the Helmholtz resonance scheme reduces the noise from 1250Hz to 3150Hz compare to original one.

1. INTRODUCTION

Rotary compressors are widely used in household air conditioners and other small refrigeration equipment, they are one of the significant sources of noise. The noise of the rotary compressor includes electromagnetic noise, mechanical noise, and aeroacoustic. Aerodynamic noise accounts for a large proportion of the rotary compressor noise in the frequency spectrum (Dreiman and Herrick, 1998). Exhaust noise is an important source of aerodynamic noise. Therefore, it is necessary to reduce it.

Exhaust noise is generated by the instantaneous release of refrigerant after compression, the expansion of gases, and the interaction with discharge valve, retainer, as well as collisions with the rough surfaces of the exhaust slope. This type of noise is characterized by its periodicity and intermittency (Sheng, 2022). Johnson (1972) specifically discussed the characteristics of the noise generated between the spatial resonance sound and the refrigerant gas discharged from the discharge valve. Jang *et al.* (2019) used the FSI technique to analysis the noise and valve behavior with and without discharge muffler, and found that a noise was generated by the internal pressure wave when the discharge valve was opened, and a vortex was generated according to the behavior of the discharge valve.

Typically, mufflers and resonant cavities around the discharge port are used to reduce the aerodynamic noise. Noguchi *et al*. (1983) analyzed the resonant frequency and sound field characteristic within the shell, and devised a special muffler. An overall noise reduction of approximately 5 d B was obtained. Sano (1983) had published a number of results on the results of a drastic reduction of noise by installing a small resonator near the discharge port.

While the mufflers are resistance silencers, they are inherently limited in their ability to suppress airflow noise within specific frequency ranges. Once these unmitigated sounds propagate, they can severely compromise the compressor's overall sonic character. Hence, the effective management of aeroacoustic sources becomes essential.

In recent years, the concept of noise reduction design based on bionic principles has gained widespread attention and development in the field of aeroacoustics. In the 1990s, Howe (1991a, 1991b) published theoretical analysis research results on noise reduction by mimicking the serrated trailing edge wing shape of owl wings, and proposed a predictive model for serrated trailing edge noise reduction. Subsequently, many scholars studied the application of serrated trailing edges in wind turbines (Dassen *et al*, 1996), compressor cascades, and open rotors (Finez *et al*, 2011. Weckmüller and Guérin, 2012. Jaron *et al*, 2018). In addition, scholars also conducted noise reduction research on wave front edges, and experimental results showed that wave front edges had good noise reduction effects (Longhouse, 1977. Hansen *et al*, 2010). Hongjun *et al* (2016) designed the V-shaped grooves on the side of the outlet of the main bearing of a rotary compressor to adjust the turbulence around the cylinder outlet, the test result showed that the V-shaped grooves could decrease the low-frequency acoustic noise.

The airflow velocity is about 20m/s~50m/s near the discharge port when the high pressure refrigerant is discharging, and the airflow impacts the wall, so it forms complex vortexes, which generates aerodynamic noise. Therefore it is necessary to reduce the noise source near the discharge port of main bearing in rotary compressors. The discharge slope is redesigned, VG, serration and Helmholtz resonance chamber structure are used to control the flow.

2. NUMERICAL METHODS AND MODELS

2.1 Numerical Method

StarCCM was used to solve the three-dimensional unsteady Reynolds-averaged Navier-Stokes equations. The volume integral and the surface flux of the diffusion terms are second-order accuracy, while the time discretization employs a second-order backward difference scheme. The k-ε turbulence model is adopted for the simulation.

A finite-volume based method is applied to solve the conservation laws for unsteady compressible flow. The Navier-Stokes equations in integral form can be written as:

$$\iiint_{C.V} \frac{\partial U}{\partial t} dV + \iint_{C.S} \vec{F} \cdot d\vec{S} = \iiint_{C.V} ST dV \quad (1)$$

Where, C.V is the control volume with boundary surface C.S. The vector of state variables U is given by:

$$U = (\rho, \rho u, \rho v, \rho w, \rho E, \rho k, \rho \varepsilon)^T \quad (2)$$

Where, ρ is the density, u, v, w are the velocity vector, and E is the total energy of the flow. The eddy viscosity is obtained from the k-ε model. The flux tensor F consists of the inviscid and viscous parts. And ST stands for the effects of gravity and other body forces.

$$\frac{\partial \rho}{\partial t} + \nabla \cdot (\rho \vec{U}) = 0 \quad (3)$$

This equation states the conservation of mass for an unsteady flow with boundaries. The momentum equation, total energy equation can be written as:

$$\frac{\partial}{\partial t}(\rho \vec{U}) + \nabla \cdot (\rho \vec{U} \times \vec{U}) = \nabla \cdot (-p\delta + \mu(\nabla \vec{U} + (\nabla \vec{U})^T)) + S_M \quad (4)$$

$$\frac{\partial}{\partial t}(\rho H) - \frac{\partial \rho}{\partial t} + \nabla \cdot \left(\rho \vec{U} H\right) = \nabla(\lambda \nabla T) + \nabla(\mu \nabla \vec{U} + \nabla \vec{U}^T - \frac{2}{3}\nabla \cdot \vec{U} \delta \vec{U}) + S_E \quad (5)$$

Where, total enthalpy H, the dynamic viscosity μ, the thermal conductivity λ, momentum source S_M, energy source S_E.

2.2 Fluid Models

Computational domain and grids are shown in Figure 1, including the inlet extension, muffler, and exhaust extension sections. A polyhedral mesh is adopted, with a total of 805,605 grid cells, and wall function y+ ≤ 50. The time step is 2.3148e-5s, corresponding to the duration for the piston to rotate 0.5 degrees. An inlet mass boundary condition is given at the straight pipe inlet (shown as Figure 2), and an average back pressure is given at the outlet of the extension section. The computational conditions are shown in Table 1.

Table 1: Boundary condition

Refrigerant	Rotate Speed/ RPS	Suction Pressure/ MPa	Discharge Pressure/ MPa	Suction Temprature/℃	Discharge Tempreture/℃
R32	60	1.018	2.861	18.3	86.8

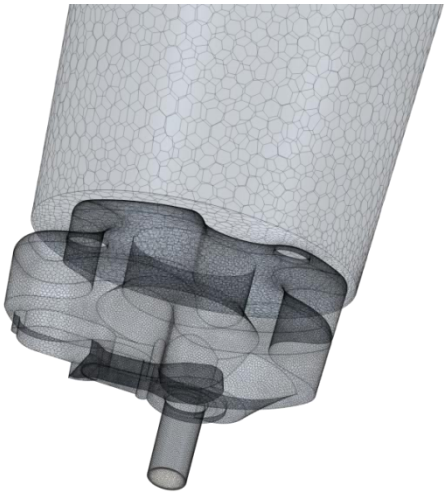

Figure 1: Models and mesh

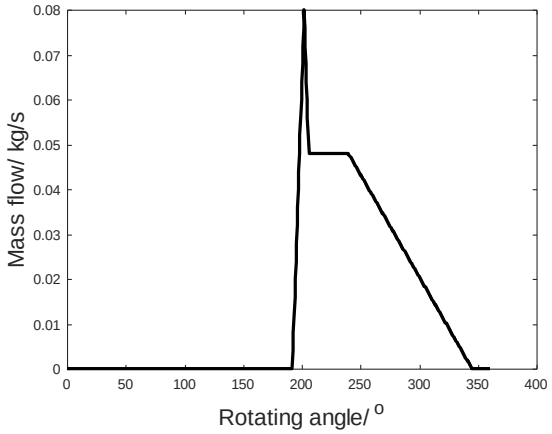

Figure 2: Inlet massflow

2.3 Design Scheme

In this study, the exhaust slopes were redesigned to investigate their impacts on noise levels. Specifically, three different design schemes were proposed, which involved adding vortex generators, serrations, and Helmholtz resonators under the exhaust slope, shown as Figure3.

(a) case with VG (b) case with serration (c) case with Helmholtz resonators

Figure 3: Geometry of upper bearing with redesigned discharge slope

3. NUMERICAL RESULT

3.1 Transmission loss of muffler

Firstly, the transmission loss of the muffler with different discharge slope was analyzed. As shown in Figure 4, after adding VG and serrations on the slope, the impact on transmission loss is minimal, with results consistent with the original plan within 3000Hz. However, the muffler has a modal at 1400Hz, there is a trough in transmission loss. To address this issue, a Helmholtz resonator under the slope is designed to enhance the transmission loss in this frequency range, thereby reducing aerodynamic noise.

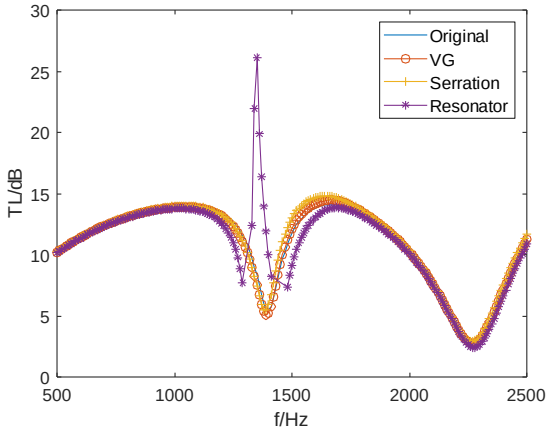

Figure 4: Transmission loss for muffler

3.2 Flow field analysis

To analyze the impact of the improvement plan on the flow field, the vorticity within the muffler is analyzed. Monitoring plane 1 and monitoring plane 2 are established at positions 0.1mm above and below the mounting surface of the muffler respectively. It can be found that the vorticity is reduced with adding VG (Vortex generator) and serration on slope from Figures 6 and 7, especially the value at the slope trailing edge part. This will help to reduce aerodynamic noise.

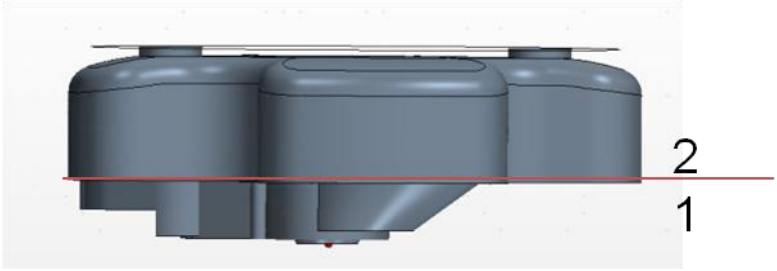

Figure 5: Monitoring surface

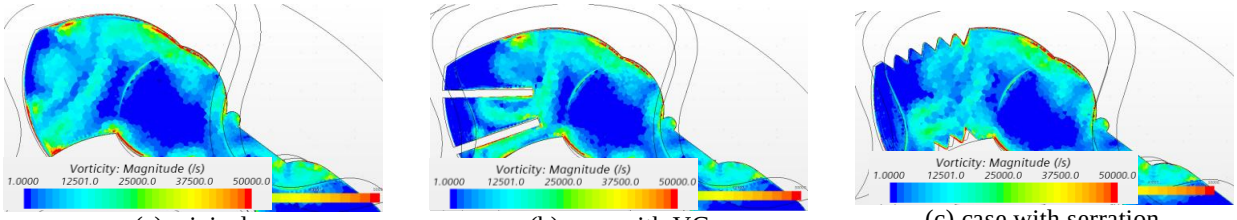

(a) original (b) case with VG (c) case with serration

Figure 6: Vorticity at plan1

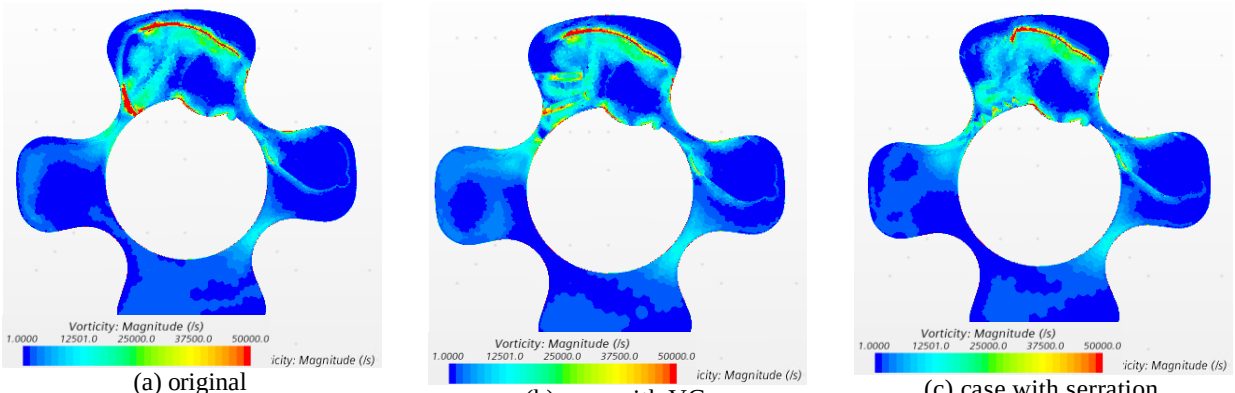

(a) original (b) case with VG (c) case with serration

Figure 7: Vorticity at plan2

3.3 Discharge pressure analysis

The central point of the muffler outlet was selected as the monitoring point. The time domain results are shown in the figure below. After adopting the improvement plan, the amplitude of the outlet pressure decreased. The Fast Fourier Transform algorithm (FFT) was used for result analysis. The sampling frequency was 4.32×10^4, with a bandwidth of 8640. A Hanning window was adopted. From Figure 9, it can be seen that after adopting the modified plan, between 200~400Hz and above 1600Hz, the exhaust pressure pulsation decreases significantly.

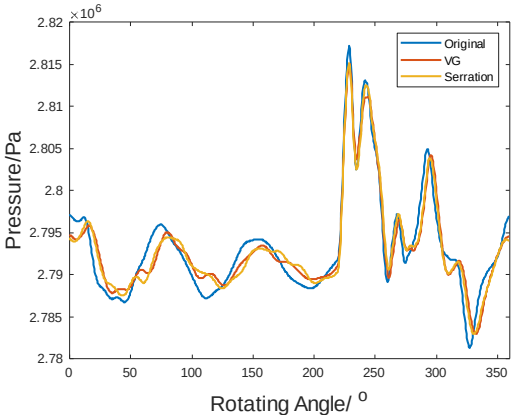

Figure 8: Discharge pressure at muffler outlet

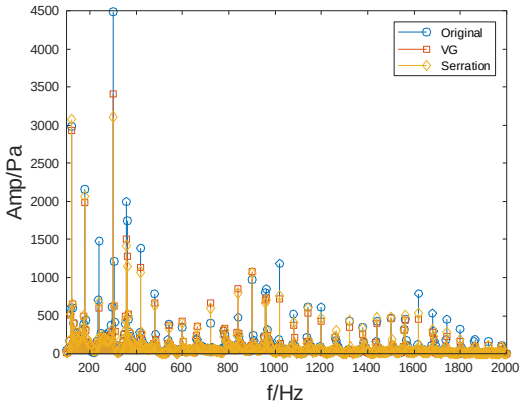

Figure 9: Discharge pressure spectrum at muffler outlet

4. EXPWRIMENT RESULTS

4.1 Acoustic response test for compressor cavity

An acoustic test rig for rotary compressor was designed (shown as Figure10). The parts of compressor can be replaced easily. The constant flow rate of gas can be injected into the compressor through the inlet pipe from a centrifugal compressor. There are 24 points on the compressor surface, used to measure sound pressure. The average pressure of all points was calculated. The results show that the compressors with VG and resonance cavity schemes have smaller responses, so the upper bearing with VG and resonance cavity were manufactured and used to assemble compressors.

4.2 Sound power test results

Acoustic power tests were conducted in a hemi-anechoic room. The microphones were 1.5 meters away from the center of the compressor. The acoustic power was tested on 3 compressors for each scheme, the average SPL and standard deviation were calculated. The test results show that the compressors with the VG scheme reduce noise by 2 dB at 1000 Hz and about 4dB above 2000 Hz, respectively; the resonance cavity scheme reduced noise by up to 5 dB between 1250 Hz and 3150 Hz. The test and simulation results are in good agreement.

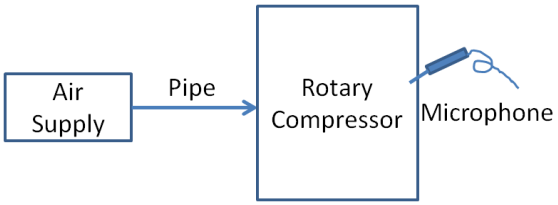

Figure 10: Acoustic response equipment

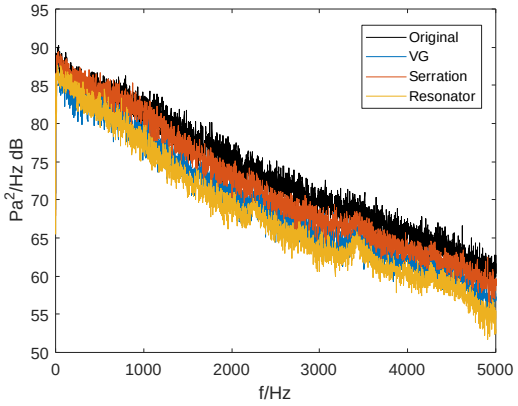

Figure 11: Average autopowers PSD

Figure 12: Sound power level test

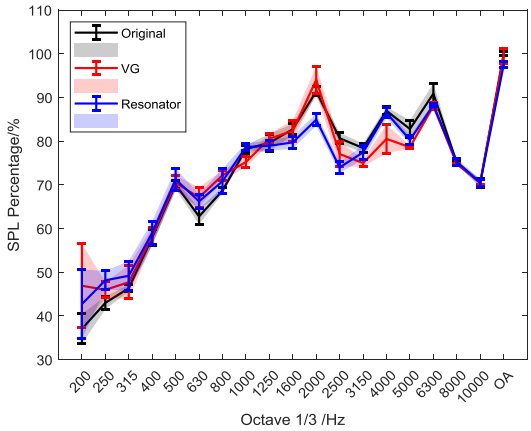

Figure 13: Sound power level Octave 1/3

5. CONCLUSIONS

As the slope of the upper bearing is a significant source of exhaust noise, VG, serration and cavity resonance were used to reduce the noise level. Simulations and tests were carried out to explore solutions.

The simulation results indicate that the VG (Vortex Generator) and serration schemes have a minimal impact on the transmission loss alteration. In contrast, the cavity resonance scheme has increased the transmission loss near 1400Hz, which corresponds to the first-order cavity modal of the muffler. Both VG

and serration schemes have successfully reduced the vorticity. The VG scheme effectively diminishes the exhaust pressure pulsations between 200~400Hz and above 1600Hz.

We selected the VG and resonant cavity schemes that showed significant effects in preliminary test. The results indicate that, the compressor using the VG scheme reduced noise by 2dB around 1000Hz and 4dB above 2000Hz. Meanwhile, the compressor employing the resonant cavity scheme achieved a maximum noise reduction of 5dB within the frequency range of 1250Hz to 3150Hz. The test and simulation results are in good agreement.

REFERENCES

Dreiman, N., & Herrick, K. (1998). Vibration and Noise Control of a Rotary Compressor.

Sheng C., (2022). Analysis and experimental study on the Aerodynamic Noise Characteristics of the Exhaust Components of Air Conditioning Compressor. Shandong University of Science and Technology

Johnson, C. N., & Hamilton, J. F. (1972). Cavity resonance in fractional horsepower refrigerant compressors.

Jang, S., Choung, H., Park, S., & Lee, S. (2019). Investigation on noise of rotary compressors using fluid-structure interaction. Journal of Mechanical Science and Technology, 33, 5129-5135.

Noguchi, M., Sano, K., & Takeshita, S. (1983). Cavity resonance and noise reduction in a rotary compressor. IEEE transactions on industry applications, (6), 1118-1123.

Masao, N. O. G. U. C. H. I. (1983). Cavity resonance and noise reduction in a compressor. IEEE Trans, 19(6), 1118-1123.

Howe, M. S. (1991). Aerodynamic noise of a serrated trailing edge. Journal of Fluids and Structures, 5(1), 33-45.

Howe, M. S. (1991). Noise produced by a sawtooth trailing edge. The Journal of the Acoustical society of America, 90(1), 482-487.

Dassen, T., Parchen, R., Bruggeman, J., & Hagg, F. (1996). Results of a wind tunnel study on the reduction of airfoil self-noise by the application of serrated blade trailing edges.

Finez, A., Jacob, M., Roger, M., & Jondeau, E. (2011, June). Broadband noise reduction of linear cascades with trailing edge serrations. In 17th AIAA/CEAS Aeroacoustics Conference (32nd AIAA Aeroacoustics Conference) (p. 2874).

Weckmüller, C., & Guérin, S. (2012). On the influence of trailing-edge serrations on open-rotor tonal noise. In 18th AIAA/CEAS Aeroacoustics Conference (33rd AIAA Aeroacoustics Conference) (p. 2124).

Jaron, R., Moreau, A., Guérin, S., & Schnell, R. (2018). Optimization of trailing-edge serrations to reduce open-rotor tonal interaction noise. Journal of Fluids Engineering, 140(2), 021201.

Longhouse, R. E. (1977). Vortex shedding noise of low tip speed, axial flow fans. Journal of sound and vibration, 53(1), 25-46.

Hansen, K., Kelso, R., & Doolan, C. (2010, June). Reduction of flow induced tonal noise through leading edge tubercle modifications. In 16th AIAA/CEAS aeroacoustics conference (p. 3700).

Hongjun C., Binsheng Z., Jiahua H. (2016). Simulation and Suppression the Rotary Compressor Acoustic Noise Base on Bionoics. 2016 China Household Electrical Appliances Technology Conference.